ELSEVIER

Journal of Crystal Growth 193 (1998) 501–509

JOURNAL OF CRYSTAL GROWTH

OMVPE growth of undoped and Si-doped GaAs epitaxial layers on Ge

Prasanta Modak[a], Mantu Kumar Hudait[a,b], Shyam Hardikar[a], S.B. Krupanidhi[b,*]

[a] *Central Research Laboratory, Bharat Electronics, Bangalore-560 013, India*
[b] *Materials Research Center, Indian Institute of Science, Bangalore-560 012, India*

Received 3 December 1997; accepted 25 June 1998

Abstract

Low-pressure organometallic vapor-phase epitaxial (LP-OMVPE) growth of undoped and Si-doped GaAs on Ge was carried out with a variation in growth temperature and growth rate. In the case of undoped and Si-doped GaAs, etch patterns showed that the epilayers consist of a single domain. Double crystal X-ray diffraction (DCXRD) indicated the compressive GaAs and the full-width at half-maxima for Si-doped GaAs decreased with increasing growth temperature. The 4.2 K photoluminescence (PL) spectrum of the undoped GaAs showed an acceptor bound excitonic peak (A^0X transition) at 1.5125 eV and the Si-doped GaAs showed two hole transitions of Si acceptors at 1.4864 eV along with the excitonic peak at 1.507 eV. This indicated the absence of Ge related peaks, i.e., (e-Ge^0_{As}) transitions. The electrochemical capacitance voltage profiler showed that the Si-doping efficiency for GaAs on Ge was less than that in GaAs on GaAs. The profiler revealed an npn structure in both the cases where the p region was in GaAs. The secondary ion mass spectroscopy (SIMS) results qualitatively indicated the absence of outdiffusion of Ge into GaAs. © 1998 Elsevier Science B.V. All rights reserved.

PACS: 78.55.Cr; 81.15.Gh; 81.70.Jb

Keywords: GaAs; Ge; OMVPE; Heteroepitaxy

1. Introduction

Heterostructure (HS) growth of GaAs epilayers on Ge substrates has received a great deal of attention because of their closely matched lattice constants and thermal expansion coefficients. GaAs solar cells offer the highest efficiency demonstrated to date for space applications [1]. GaAs substrates are somewhat fragile and thus the cell thickness must be appreciable in order to be durable. On the other hand, Ge possesses shallow impurity levels and is a very rugged material so that it can be thinned to reduce overall cell weight without introducing any mechanical problem. In terms of power-to-weight ratio, GaAs on Ge can outperform GaAs on GaAs solar cells in space applications [1].

* Corresponding author. Fax: + 91 80 3341683; e-mail: sbk@mrc.iisc.ernet.in.

0022-0248/98/$ – see front matter © 1998 Elsevier Science B.V. All rights reserved.
PII: S0022-0248(98)00600-9

Furthermore, the reverse breakdown voltage of GaAs cells grown on Ge substrates is lower than that of GaAs cells grown on GaAs substrates, which can reduce the cell degradation caused by large reverse currents [2].

The use of Ge instead of GaAs substrates raises several interesting material growth issues, like, the growth of polar semiconductors on nonpolar substrates, GaAs doping by Ge and Ge doping by Ga and As. The slight charge imbalance between the covalent Ge and slightly ionic GaAs has been reported to form antiphase domains (APDs) which are small areas resembling polycrystalline grains that reduce the electronic quality of GaAs layers grown on Ge [3]. The problem of APDs can be solved by the use of Ge substrates misoriented a few degrees away from (1 0 0) towards (1 1 0) direction [4]. Mizuguchi et al. [4] report the successful growth of single domain epi-GaAs on Ge(1 0 0) 2° off towards [0 1 1] at a temperature of 720°C and a growth rate of 0.03 μm/min. Li et al. [5] report that for a Ge(1 0 0) substrate misoriented towards (1 1 0) by an angle of less than 3°, APDs were present for a low-pressure organometallic vapor-phase epitaxy (LP-OMVPE) growth at 700°C, however, a 4 μm thick layer was found necessary to annihilate the APDs. They also identified a minimum arsine partial pressure of 2 mbar, a reasonably high growth temperature and a relatively low growth rate necessary to ensure APD-free epitaxy of GaAs on Ge. Timó et al. [6] report that a higher growth rate (10 μm/h) gives a better surface morphology. Also, it was found that the interdiffusion was probably much more effective in the case of lower growth rate (2 μm/h) due to the longer time needed to grow the epifilms.

The indiffusion of Ga and As into Ge during the GaAs cell growth creates a p–n junction in the Ge [7]. At the typical growth temperature, Ga has higher solid solubility and lower diffusion coefficient than that of As. Therefore, the p-type dopant Ga diffuses into the Ge for a shorter distance during the growth duration and compensates the diffusing As from the GaAs and the already present dopant in the Ge wafer, both of which are n-type dopants. This results in a shallow p–n junction (called active-Ge), just below the GaAs epilayer that contributes extra photovoltage in cascade with the GaAs p/n junction [8]. This active-Ge junction does not provide any extra power output and, in fact, reduces the total efficiency under the AM0 condition [9]. In order to suppress the active Ge junction, a combination of slower growth rate combined with a lower initial nucleation temperature has been suggested to consistently change the GaAs on Ge interface density and/or reduce the interdiffusion of Ga, As and Ge [9].

Evidently, GaAs layer growth conditions on Ge involve a complex trade off between various factors namely, the use of optimum crystal orientation in the Ge substrates, choice of optimum growth temperatures not only for the interface layers but also for the upper GaAs layers. Thus, it appears that there exists no unique growth procedure that will ensure APD free passive GaAs on Ge junction with good surface morphology. In this paper, we report the effect of LP-OMVPE growth conditions on the interface properties of the undoped and Si-doped epilayers of GaAs on vicinal Ge substrates. Results will be presented in close correlation with growth conditions.

2. Experimental details

Growth of undoped and Si-doped epitaxial GaAs layers was carried out in a horizontal low-pressure organometallic vapor-phase epitaxy (LP-OMVPE) reactor at 100 Torr using high purity hydrogen as the carrier gas with trimethylgallium (TMG) and 100% arsine (AsH_3) as the group III and group V sources, respectively. Silicon doping was carried out by using silane (SiH_4) diluted to 104 ppm in hydrogen as an n-type dopant precursor. Both the Sb-doped (1×10^{17} cm^{-3}) Ge substrates of (1 0 0) orientation 6° off towards ⟨1 1 0⟩ and Si-doped (1×10^{18} cm^{-3}) n^+ GaAs substrates of (1 0 0) orientation 2° off towards ⟨1 1 0⟩ were used in the same run for the growth process. Details of the growth procedure can be found elsewhere [10]. Doping studies were carried out with a variation in temperature from 600 to 700°C and TMG mole fraction was varied between 8.92×10^{-5} and 2.67×10^{-4}.

The A–B etch technique was employed in order to find out evidence for APDs. The epitaxy of

undoped and Si-doped GaAs layers were confirmed by double crystal X-ray diffraction (DCXRD) studies. Low-temperature photoluminescence (LTPL) measurements were carried out at 4.2 K with a 100 mW argon ion laser operating at a wavelength of 5145 Å as a source of excitation. The PL signal was detected by a LN_2 cooled Ge-photodetector whose operating range is about 0.75–1.9 eV, with the resolution being kept at 0.5 meV. By employing the electrochemical CV (ECV) profiler, detailed studies were carried out for the epi-GaAs on Ge interface. The data for epi-GaAs grown on GaAs has been presented for a better understanding of the growth process. Secondary ion mass spectroscopy (SIMS) data was used in order to correlate our results regarding interdiffusion of Ga and As into Ge and that of Ge into GaAs. SIMS was carried out using Cs^+ ions as the primary ion source with an acceleration energy of 10 keV.

3. Results and discussion

3.1. A–B etch patterns

The A–B etch revealed the etch pits in our samples and a typical pattern can be seen from Fig. 1. Our figure shows a typical etch pattern of an epitaxial GaAs layer and indicates the absence of any hexagonal etch pits at right angles. All the etch pits have the same direction [4] within the GaAs layer on the whole Ge substrate. This result confirms that the GaAs layers grown on 6° off oriented (1 0 0) toward the (1 1 0) Ge substrate consisted of a single domain. It is suggested [11] that As and Ga each nucleate preferentially at one of the two different step sites available on the vicinal Ge substrate surface. After the As prelayer, the Ga adatoms will exchange sites with As atoms to occupy the step sites for which it is energetically favorable. Thus, the step will propagate along the terrace as Ga atoms exchange with As atoms at the step site. This will continue until the next step is reached, at which point the lattice will be in registry and single domain material is achieved.

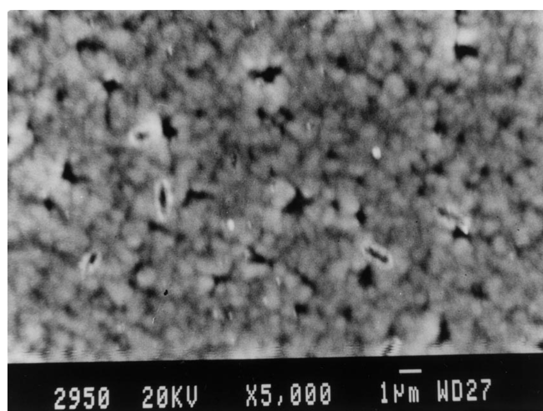

Fig. 1. SEM micrograph of a typical A–B etch pattern of epi-GaAs on Ge.

3.2. Double crystal X-ray diffraction studies

In order to confirm the epitaxial nature of the growth, undoped GaAs on Ge were grown before growing the Si-doped GaAs on Ge. Fig. 2a shows a DCXRD curve for an undoped epilayer of GaAs grown on Ge at a temperature of 625°C and at a growth rate of 4 μm/h. The GaAs epilayer peak with a FWHM of 45 arcsec appears on the right-hand side of the Ge peak which is in accord with the fact that the GaAs epilayer lattice constant is higher than that of the Ge. In case of Si-doped GaAs on Ge, we observed a reduction in full-width at half-maximum (FWHM) with growth temperature and this can be seen from Fig. 2b. This may be due to slips occurring as a result of plastic deformation when the stress due to differential thermal expansion exceeds the critical yield stress for Ge. Calculations for ($\delta a/a$) showed that the GaAs epilayers were compressive in nature where the compression initially increased and then decreased after a growth temperature of 700°C. The compression of the lattice along the depth may be due to elastic deformation that may be caused by the stretching of the lattice along the surface because of the difference of thermal shrinkage between GaAs epitaxial layer and substrates [4]. This shows that at least for some purposes, it is wrong to assume that the small differences between the lattice constants and thermal expansion coefficients of Ge and GaAs can be neglected [12]. No information on the diffusion effects could be obtained since the layer thickness was larger than critical thickness (t_c), which is between 290 to 450 nm [6].

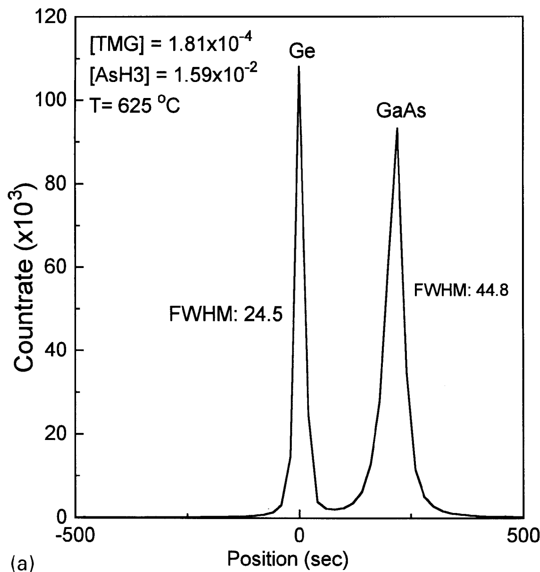

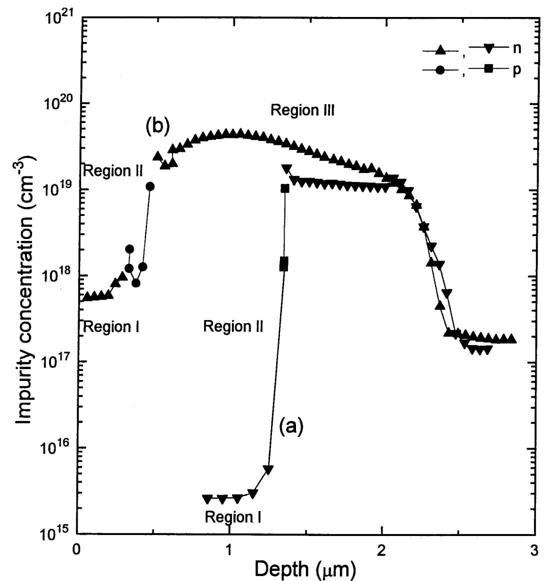

Fig. 3. Electrochemical capacitance voltage profile of (a) undoped and (b) Si-doped GaAs on Ge showing three regions (I, II, and III). Growth parameters for the undoped GaAs are: [TMG] $= 1.81\times10^{-4}$, [AsH_3] $= 1.59\times10^{-2}$, $T = 625$°C and for the doped GaAs: [TMG] $= 1.78\times10^{-4}$, [AsH_3] $=$ 1.57×10^{-2}, [SiH_4] $= 5.79\times10^{-7}$, $T = 675$°C.

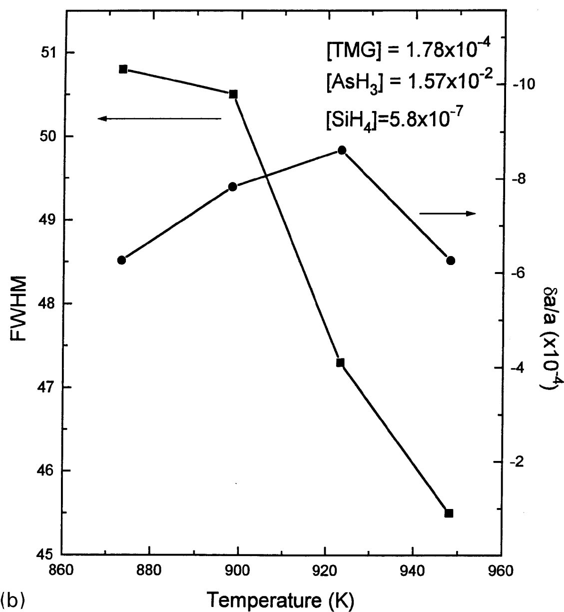

Fig. 2. DCXRD plot of (a) a undoped GaAs on Ge and (b) variation of FWHM and compression with growth temperature for Si-doped GaAs on Ge.

3.3. Photoluminescence measurements

3.3.1. Undoped and Si-doped GaAs/Ge

The photoluminescence studies have been carried out on both the undoped and doped epi-GaAs at the sample surface and after etching some thickness of the epilayer as per the regions defined in Fig. 3. Region I corresponds to the n-type epilayer GaAs, region II is a p-type GaAs and the region III is a Ge substrate.

For the undoped GaAs, PL spectra (Fig. 4a) from region I showed an acceptor bound excitonic peak (A^0X transition) at 1.5125 eV with a full-width at half-maximum (FWHM) of around 15.1 meV. The photoluminescence spectrum corresponding to region II for undoped GaAs was taken after etching about 1.3 μm showed a peak at 1.516 eV with a FWHM of 13.2 meV which corresponds to the free excitonic emission [13]. The PL free excitonic peak of region II (Fig. 4b) was of higher energy and lower intensity than the excitonic peak of region I. Masselink et al. [14] have observed that in the case of GaAs grown on Ge, the dominant photoluminescence feature is a single peak whose maximum lies between 1.477 and 1.473 eV depending on the excitation intensity. This luminescence was due to the e-Ge^0_{As} and Ge^0_{Ga}–Ge^0_{As} (free electron to

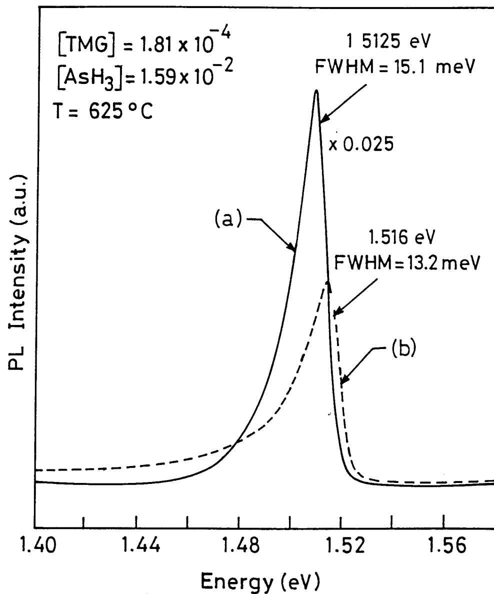

Fig. 4. 4.2 K photoluminescence of undoped GaAs on Ge (a) at the surface (continuous line) and (b) after etching about 1.3 μm (dashed line).

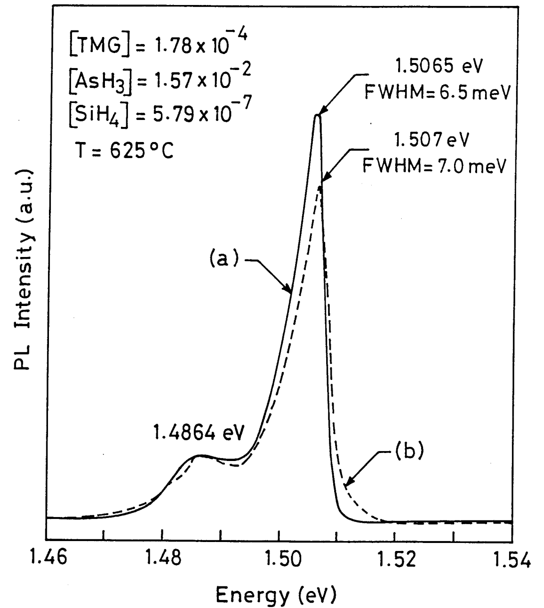

Fig. 5. 4.2 K photoluminescence of Si-doped GaAs on Ge (a) at the surface (continuous line) and (b) after etching about 0.8 μm (dashed line).

acceptor and donor to acceptor) transition involving the Ge acceptor and donor and had a phonon replica at 1.437 eV. This would indicate a binding energy of 43 meV for the Ge acceptor in GaAs. They also observed a luminescence from the recombination of bound exciton at 1.511 eV [15]. However, our present data does not show any such peaks either at the undoped GaAs epilayer surface or at the GaAs/Ge interface where the GaAs is p-type. This confirms that there was no Ge outdiffusion into GaAs during our present growth condition.

In case of Si-doped GaAs on Ge, the PL spectra (Fig. 5a) for the surface of the epi-GaAs showed two hole transition of Si acceptor levels corresponding to an energy level of 1.4864 eV [15] along with the excitonic peak at 1.5065 eV with a FWHM of 6.5 meV. The PL spectrum for region II (Fig. 5b) showed similar peaks at 1.4864 eV and the excitonic peak at 1.507 eV with a FWHM of 7.0 meV as we obtained in case of region I. As is evident, the excitonic peak intensity from region I is more than that from region II. This PL spectrum suggests that there is no Ge out diffusion from the substrate for a growth rate of 4 μm/h. Timó et al. [6] however, obtained massive outdiffusion of Ge into GaAs at lower growth rates (2 μm/h) and did not observe any outdiffusion of Ge at higher growth rates (10 μm/h).

3.3.2. Effect of growth temperatures and the growth rate on photoluminescence

The PL spectra shifts towards higher energy with growth temperature (Table 1a), and with TMG mole fractions on Ge substrates, whereas the PL spectra shifts towards higher energy with growth temperature and shifts to lower energy with TMG mole fractions on GaAs substrates. The shift in PL peak energy towards the higher energy is due to the increase in electron concentration and can be ascribed to Burstein–Moss shift [16,17]. The Burstein–Moss shift is more pronounced when the electron concentration increases in the epitaxial Si-doped GaAs layers. The peak energies for GaAs/GaAs are higher than that of GaAs/Ge in case of both the growth temperature and growth rate variations. Thus, the free electron concentration would be less in epi-GaAs on Ge substrates than that on

Table 1

(a) Variation of 4.2 K photoluminescence FWHM and peak energy with growth temperature and TMG mole fraction for Si-doped GaAs on Ge and GaAs on GaAs. Growth parameters are: $[AsH_3] = 1.57 \times 10^{-2}$ and $[SiH_4] = 5.18 \times 10^{-7}$

TMG mole fraction	Growth temperature (°C)	PL FWHM (eV)		PL peak energy (eV)	
		GaAs/Ge	GaAs/GaAs	GaAs/Ge	GaAs/GaAs
1.78×10^{-4}	675	15.6	17.3	1.512	1.5199
1.78×10^{-4}	650	9.5	6.9	1.5081	1.5172
1.78×10^{-4}	625	5.8	5.7	1.5065	1.5177
1.78×10^{-4}	600	5.7	5.2	1.5062	1.5158
8.92×10^{-5}	650	14.1	10.7	1.5081	1.5206
1.78×10^{-4}	650	9.5	6.9	1.5081	1.5172
2.67×10^{-4}	650	16.5	5.5	1.5117	1.5163

(b) Variation of free electron concentration with TMG mole fraction for Si-doped GaAs on Ge and GaAs on GaAs. Growth parameters are: $[AsH_3] = 1.57 \times 10^{-2}$, $[SiH_4] = 5.18 \times 10^{-7}$ and $T = 650°C$

TMG mole fraction	Doping concentration (cm^{-3})	
	GaAs/Ge	GaAs/GaAs
8.92×10^{-5}	1.96×10^{17}	4.0×10^{17}
1.78×10^{-4}	2.3×10^{17}	3.64×10^{17}
2.67×10^{-4}	2.75×10^{17}	3.10×10^{17}

GaAs substrates. The FWHM of the B–B (band-to-band) peak at 4.2 K of PL spectra for epi-GaAs increases with increasing growth temperature in case of both the Ge and GaAs substrates. The FWHM increases with increasing TMG mole fraction in Ge substrates but decreases in GaAs substrates. The detailed discussion can be found elsewhere [18].

3.4. Electrochemical capacitance voltage profiles

3.4.1. Effect of growth temperature and growth rate on impurity incorporation

To find out the doping efficiency of Si-doped GaAs on Ge in comparison with that of GaAs on GaAs, growth temperature was varied under fixed SiH_4 mole fraction and the impurity profile was measured by employing the ECV profiler. The impurity concentration was less in GaAs grown on Ge compared to the GaAs grown on GaAs substrate as can be seen from Fig. 6. The possible explanation for the increase in electron concentration in GaAs grown on GaAs substrate than on Ge substrates in our case is the catalyzed pyrolysis of SiH_4 by the presence of a GaAs surface [19] or the polar and nonpolar nature of the substrates may influence the silicon incorporation. The difference in electron concentration in the GaAs grown on Ge and GaAs substrate could be the traps in the GaAs epilayer due to the defects originating from the hetero-epitaxy [20]. GaAs can be grown epitaxially on Ge in two equivalent orientations corresponding to an exchange of the Ga and As sublattices. Since GaAs is a polar material, the APBs have a net charge and are expected to act as scattering centers [11]. Anti-phase boundaries in GaAs contains Ga–Ga and As–As bonds. Such bonds represent electrically charged defects, which may trap electrons. This explanation becomes less likely because we have not observed the presence of APDs in the present case. Also at higher electron concentrations of the order of 10^{17} cm^{-3} obtained in our doped films, the

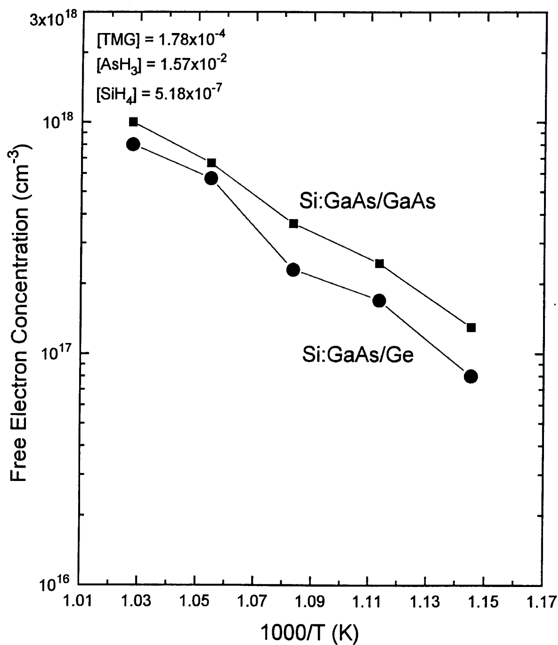

Fig. 6. Variation of Si doping concentration in GaAs on Ge with growth temperature. The data for GaAs on GaAs is included for reference.

reduction in the doping due to traps may not be valid due to the required very high trap concentrations [21]. Sieg et al. [21] observed identical Si-doping efficiencies on both Ge and GaAs substrates at least at low doping levels ($2.5 \times 10^{15}\ cm^{-3}$) grown by solid source molecular beam epitaxy (MBE) technique. They also suggested that for MBE films, Ge out diffusion into the GaAs is an unlikely cause of the reduced apparent Si-doping efficiency, since Ge usually produces n-type doping in GaAs. Besides, we have not observed any PL peaks in our samples in between 1.473 and 1.477 eV indicative of the e-Ge^0_{As} and Ge^0_{Ga}–Ge^0_{As} (free electron-to-acceptor and donor-to-acceptor) transition involving Ge acceptor and donor [14]. These results thus rule out the possibility of Ge outdiffusion into GaAs during our present growth conditions.

Table 1b lists the growth rate dependence of Si incorporation in epi-GaAs on both the Ge and GaAs substrates. It was found that, with increasing TMG flow rate, i.e., increasing growth rate, the free electron concentration increases in the epi-GaAs on Ge. The increase in Si doping with increasing growth rate in GaAs on Ge may also be explained by the enhanced SiH_4 pyrolysis in the vicinal Ge substrate. The free electron concentration was found to decrease with increasing growth rate in the epi-GaAs on GaAs. This is similar to the result obtained by Bass [22] and Sakaguchi et al. [23].

3.4.2. Analysis of carrier concentration profile

As shown in the Fig. 3, the ECV plot for both the undoped (Fig. 3a) and doped (Fig. 3b) GaAs on Ge, there are three clearly defined regions. Region I corresponds to the surface of the GaAs epilayer that is n-type. Region II is of p-type conductivity and from the results of the photovoltage spectrum (not shown), this is epi-GaAs. Region III is an n-type Ge substrate; we observed that this part of the substrate adjacent to the GaAs epilayer is heavily doped with As in the range of $10^{19}\ cm^{-3}$, essentially because the Sb dopant already existing in the Ge substrate gives a doping concentration of only $1 \times 10^{17}\ cm^{-3}$. Similar As diffusion profile into Ge has been observed by Tobin et al. [24] by employing a spreading resistance technique in a GaAs on Ge tandem solar cell. Chand et al. [25] report thyristor-like npnp structure for MBE growth of n-GaAs on p-Ge substrate. They proposed that Ge from the substrate outdiffuses into the growing GaAs layer and As from the GaAs into the Ge substrate inverting the Ge surface from p to n type. The Ge, which will occupy As vacancy sites in GaAs, would behave as a p dopant in GaAs [24]. This phenomenon will result in an npnp thyristor-like structure as proved by their electrical and optical characteristics. We also observed the formation of a p-type GaAs at GaAs/Ge heterointerface in case of both the undoped and doped GaAs. However, the PL results do not show any Ge acceptor related peaks at 1.473 eV [14] from p-GaAs regions. Appropriate discussion may be found in Section 3.3.1. The fomation of p-GaAs thus cannot be attributed to the Ge acceptors. Further studies are in progress to determine the exact nature of the p-GaAs region.

3.5. SIMS analysis

In order to verify the interdiffusion of Ga and As into Ge and the outdiffusion of Ge into GaAs,

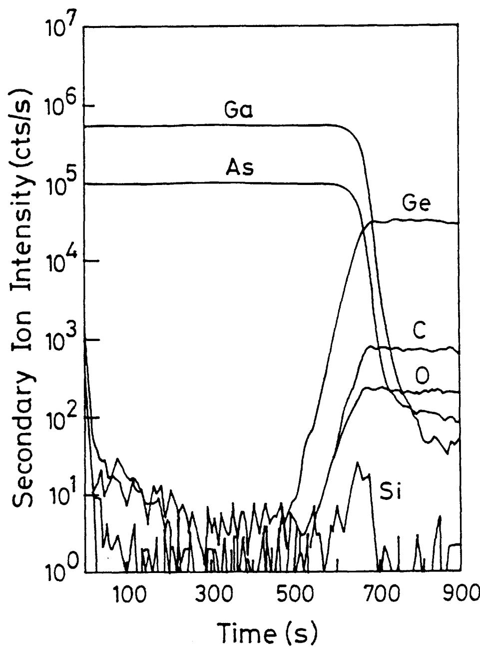

Fig. 7. SIMS depth profile of compositional atoms for epi-GaAs on Ge.

a physical method namely, secondary ion mass spectroscopy (SIMS) technique was used. This technique yields quantitative measurements of dopants and impurity levels in semiconductors. In the dynamic SIMS technique, the mass spectral peak intensity corresponding to a particular ion is monitored as a function of time using a high sputtering rate. Fig. 7 shows depth profiles (sputter rate ≈ 15 Å/s) of Ga, As, Ge, C, Si, and O atoms in the Si-doped GaAs on Ge, measured by SIMS for a TMGa mole fraction of 1.78×10^{-4}. Clearly, there is little or no outdiffusion of Ge [26,27] at the heterointerface of the GaAs on Ge(1 0 0) substrate. The abrupt heterointerface in this film qualitatively indicates the almost no outdiffusion of Ge into the GaAs epifilm. These studies are in agreement with the results obtained from PL studies as shown in Figs. 4 and 5.

4. Conclusions

Epitaxial growth of undoped and Si-doped GaAs on Ge by LP-OMVPE technique has been carried out. The A–B etch pattern clearly indicated that all etch pits have the same orientation within the GaAs layer on the whole Ge substrate. This result confirmed that the GaAs layers grown on 6° off (1 0 0) toward (1 1 0) Ge substrates are APD free and thus consist of a single domain. The DCXRD data showed slightly compressive GaAs on Ge that initially increased and then decreased with increasing growth temperature. The LTPL measurements confirmed the epitaxy and showed no Ge related peaks, i.e. (e-Ge^0_{As}) transitions indicating the absence of Ge outdiffusion into the epifilm. The electrochemical CV data showed that Si-doping efficiency in GaAs on Ge was lower than that in the GaAs on GaAs system. This may possibly be explained by the catalyzed pyrolysis of SiH_4 by the presence of a GaAs surface or the polar and nonpolar nature of the growth may influence the silicon incorporation. The impurity profile further revealed an npn structure for undoped and doped GaAs where the p-type conductivity was observed at the GaAs on Ge heterointerface. The SIMS data qualitatively indicated little or no Ge out-diffusion into the epifilm.

Acknowledgements

The authors wish to thank Prof. D.N. Bose and Mr. Satyabhan at I.I.T., Kharagpur, India for DCXRD data, Ms. P. Indira for carrying out the A–B etch experiments. We also thank Dr. K.S.R.K. Rao for the PL measurement and Mr. R. Ashwatraman, Kalpakkam (IGCAR) for the SIMS analysis.

References

[1] K.I. Chang, Y.C.M. Yeh, P.A. Iles, J.M. Tracy, R.K. Morris, 19th IEEE Photovoltaic Specialists Conf. Issue, 1987, p. 273.

[2] J.C. Chen, M. Ladle Ristow, J.I. Cubbage, J.G. Werthen, 22nd IEEE Photovoltaic Specialists Conf. Issue, 1991, p. 133.

[3] Y.C.M. Yeh, K.I. Chang, C.H. Cheng, F. Ho, P.A. Iles, 20th IEEE Photovoltaic Specialists Conf. Issue, 1988, p. 451.

[4] K. Mizuguchi, N. Hayafuji, S. Ochi, T. Murotani, K. Fujikawa, J. Crystal Growth 77 (1986) 509.

[5] Yuan Li, G. Salviati, M.M.G. Bongers, L. Lazzarini, L. Nasi, L.J. Gilling, J. Crystal Growth 163 (1996) 195.
[6] G. Timó, C. Flores, D. Passoni, C. Bocchi, P. Franzosi, L. Lazzarini, G. Salviati, J. Crystal Growth 125 (1992) 440.
[7] S.P. Tobin, S.M. Vernon, C. Bajgar, V.E. Haven Jr., S.E. Davis, 18th IEEE Photovoltaic Specialists Conf. Issue, 1985, p. 134.
[8] S.J. Wojtczuk, S.P. Tobin, C.J. Keavney, C. Bajgar, M.M. Sanfacon, L.M. Geoffroy, T.M. Dixon, S.M. Vernon, J.D. Scofield, D.S. Ruby, IEEE Electron Device Lett. EDL-37 (1990) 455.
[9] P.A. Iles, Y.C.M. Yeh, F.H. Ho, C. Chu, C. Cheng, IEEE Electron Device Lett. EDL-11 (1990) 140.
[10] P. Modak, M.K. Hudait, S.B. Krupanidhi, Conf. Proc. Int. Workshop on Physics of Semiconductor Devices, 1995, p. 361.
[11] S. Strite, D. Biswas, N.S. Kumar, M. Fradkin, H. Morkoc, Appl. Phys. Lett. 56 (1990) 244.
[12] Djula Eres, D.H. Lowndes, J.Z. Tischler, J.W. Sharp, T.E. Haynes, M.F. Chisholm, J. Appl. Phys. 67 (1990) 1361.
[13] L Pavesi, M Guzzi, J. Appl. Phys. 75 (1984) 4779.
[14] W.T. Masselink, R. Fischer, J. Klem, T. Henderson, P. Pearah, H. Morkoc, Appl. Phys. Lett. 45 (1984) 457.
[15] R. Fischer, W.T. Masselink, J. Klem, T. Henderson, T.C. McGlinn, M.V. Klein, H. Morkoc, J. Appl. Phys. 58 (1985) 374.
[16] E. Burstein, Phys. Rev. 93 (1954) 632.
[17] T.S. Moss, Proc. Phys. Soc. London, Sect. B 67 (1954) 775.
[18] M.K. Hudait, P. Modak, S. Hardikar, S.B. Krupanidhi, J. Appl. Phys. 83 (1998) 4454.
[19] G.B. Stringfellow, in: Organometallic Vapor-Phase Epitaxy, Theory and Practice, Academic Press, 1989, p. 170.
[20] Herbert Kroemer, J. Crystal Growth 81 (1987) 193.
[21] R.M. Sieg, S.A. Ringel, S.M. Ting, E.A. Fitzgerald, J. Electron. Mater. (1997), in press.
[22] S.J. Bass, J. Crystal Growth 47 (1979) 613.
[23] H. Sakaguchi, R. Suzuki, T. Meguro, J. Crystal Growth 93 (1988) 602.
[24] S.P. Tobin, S.M. Vernon, C. Bajgar, V.E. Haven, L.M. Geoffroy, D.R. Lillington, IEEE Electron Device Lett. EDL-9 (1988) 256.
[25] N. Chand, J. Klem, T. Henderson, H. Morkoc, J. Appl. Phys. 59 (1986) 3601.
[26] T. Kawai, H. Yonezu, H. Yoshida, K. Pak, Appl. Phys. Lett. 61 (1992) 1216.
[27] T. Kawai, H. Yonezu, Y. Yamauchi, M. Lopez, K. Pak, J. Crystal Growth 127 (1993) 107.